A Functionalizable Analog of the Yariv Reagent for AGP Imaging using Fluorescence Microscopy

Sebastian Rueda[†], Tyler J. McCubbin[‡], Meg Shieh[†], Raghuraj Hoshing[†], David M. Braun[‡ §], Amit Basu[†*]

[†] Department of Chemistry, Brown University, Providence, RI 02912, USA

[‡] Division of Plant Science and Technology, Interdisciplinary Plant Group, The Missouri Maize Center, University of Missouri, Columbia, MO 65211, USA

[§] Division of Biological Sciences, University of Missouri, Columbia, MO 65211, USA

* *abasu@brown.edu*

Abstract

Small molecule fluorescent probes that bind selectively to plant cell wall polysaccharides have been instrumental in elucidating the localization and function of these glycans. Arabinogalactan proteins (AGPs) are cell wall proteoglycans implicated in essential functions such as cell signaling, plant growth, and programmed cell death. There is currently no small molecule probe capable of fluorescently labeling AGPs. The Yariv reagents are the only small molecules that bind AGPs, and have been used to study AGP function and isolate AGPs via precipitation of an AGP-Yariv complex. However, the Yariv reagents are not fluorescent, rendering them ineffective for localization studies using fluorescence microscopy. A fluorescent version of a Yariv reagent that is capable of both binding as well as imaging AGPs would provide a powerful tool for studying AGPs *in planta*. Herein, we describe the synthesis of an azido analog of the Yariv reagent that can be further functionalized with a fluorophore to provide a glycoconjugate that binds AGPs and is fluorescent. We show that the modified reagent binds gum arabic in *in vitro* binding assays when used in conjunction with the βGlcYariv reagent. Fluorescent imaging of AGPs in fixed maize leaf tissue enables localization of AGPs to cell walls in the leaf. Significantly, imaging can also be carried out using fresh tissue. This represents the first small molecule probe that can be used to visualize AGPs using fluorescence microscopy.

Keywords

Plant Cell Wall, Click Chemistry, Polysaccharide, Arabinogalactan, Dye, Glycoconjugate

Introduction

Plant cell walls are comprised of an intricate assembly of polysaccharides including cellulose, hemicelluloses, and pectins, along with crosslinked lignins and proteoglycans such as arabinogalactan proteins (AGPs).[1–4] There is a pressing need for the development of tools that can image the complex and dynamic plant cell wall.[5–8] Fluorescence microscopy is a powerful method for visualizing components of the plant cell wall because of its high sensitivity and spatial resolution. Small molecule fluorescent dyes are vital compounds in elucidating the distribution of these components. For example, Sirofluor and Calcofluor White (Figure 1) are commonly used as fluorescent stains for callose and cellulose, respectively. However, not all cell wall components have corresponding small molecule fluorescent probes that can be used for imaging. We report here the result of our efforts to develop a method for fluorescently imaging AGPs using small molecules.

AGPs are proteoglycans found throughout the plant, including in leaves, roots, stems, pollen tubes, and pollen grains.[9] AGPs are implicated in myriad functions ranging from plant growth, cellular signaling, programmed cell death, and many others.[10–12] AGPs contain protein domains rich in hydroxyproline residues that are glycosylated with long β(1→3)-linked galactan chains that make up the bulk of AGP mass.[13,14] Shorter branching β(1→6) galactan side chains are linked from the galactan main chains and are commonly decorated with arabinofuranose residues and other monosaccharides, with variations in the specific composition of the branches depending on the species and plant tissue.

There are currently two methods for investigating the localization of AGPs *in planta* – immunofluorescence using monoclonal antibodies (MAbs), and the set of dyes known as the Yariv reagents (*vide infra*).[9] While MAbs can provide bright images showing AGP decoration, they are

highly epitope specific, and due to their large size, the antibodies may not be able to access all parts of the cell wall.[6,8] On the other hand, the Yariv reagents, dyes based on a tri-glycosylated phloroglucinol core (Fig. 1), bind AGPs but can only be visualized using the less sensitive brightfield microscopy. The AGP binding ability of the Yariv reagents depends on the structure of the sugar moieties attached to the aromatic core.[15,16] Yariv reagents bearing β-D linked glucose (βGlcYariv) or galactose bind strongly to AGPs and have been used to isolate AGPs from plants by precipitation of an AGP-Yariv complex.[17–19] Yariv reagents comprised of α-linked sugars or L sugars do not bind to AGPs. The Yariv reagents aggregate in solution and bind to the core β(1→3)-linked galactan backbone, which is postulated to be helical.[20,21] We have used circular dichroism (CD) spectroscopy to show that the Yariv reagent aggregates are also helical, and that the sense and magnitude of helicity correlates with AGP binding ability.[16] The Yariv reagents are exceptionally selective for AGPs and do not bind strongly to other polysaccharides present in the plant cell wall. Given the specificity of Yariv reagents for AGPs, they are an excellent scaffold for designing a fluorescent probe for this important cell wall component.

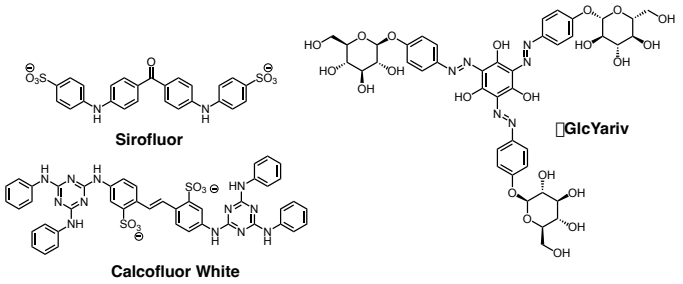

Figure 1 – Small molecule plant cell wall probes

In this work, we describe the first synthesis and use of a fluorescent version of a Yariv reagent, prepared using an azido analog of the parent Yariv reagent (**AzYariv**) as a key intermediate. Modification of **AzYariv** with an alkyne-linked fluorophore provides the target glycoconjugate. The modified Yariv reagent binds to AGPs in vitro using an agarose reverse gel

assay. Most importantly, experiments using the fluorescently tagged Yariv reagent with maize leaves demonstrate the ability to visualize AGPs using fluorescence microscopy. These results validate the utility of the new probe for studying AGPs, and provide an opportunity for researchers to carry out more sophisticated imaging of AGP localization and function *in planta*.

Results & Discussion

*Synthesis and Characterization of **AzYariv***

Our design of a fluorescent Yariv reagent was guided by the observation that the Yariv reagent prepared from 6-methoxy-D-glucose retains the ability to bind AGPs, while other analogs such as the 2-methoxy-D-glucose or L-glucose derivatives do not bind.[15] This suggested that the 6-position on a β-D-glucosyl residue could serve as the attachment point for a fluorescent chromophore. We also sought a linkage chemistry that would undergo facile functionalization and allow for a simple purification and isolation of the dye-adduct. The use of a 6-azido substituent was considered ideal as the azide can be readily functionalized via click reactions with alkynes, especially cyclooctynes.[22] This is of particular interest as the strain-promoted azide alkyne cycloaddition (SPAAC) of cyclooctynes does not require the presence of additional reagents which would need to be separated from the final adduct. Additionally, the absence of copper, which can be toxic to plants,[23] is a further advantage of the SPAAC. Finally, reports of mixed Yariv reagents, where one of the glucosyl residues was substituted with another sugar or even a *p*-nitroaniline without complete loss of AGP binding suggested that introduction of a single azido sugar substitution should not be deleterious.[15] Thus, we set out to synthesize an azido analog of

βGlcYariv in which one of the glucosyl units has been replaced by a 6-deoxy-6-azido β-D-glucosyl residue (**AzYariv**, Scheme 1).

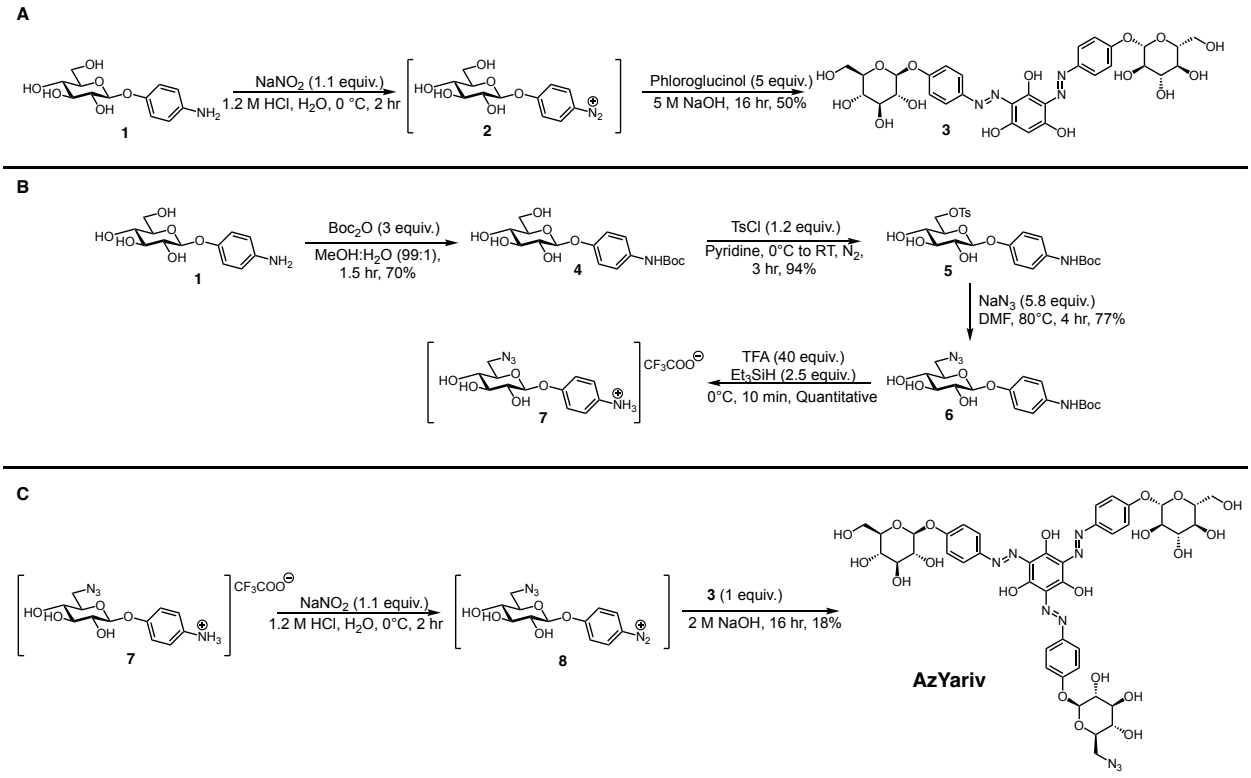

Scheme 1 – Syntheses of **A) 3**; **B) 7**; **C) AzYariv** reagent.

In order to synthesize **AzYariv**, we required the bis-glucosylated phloroglucinol adduct **3** as an intermediate (Scheme 1, A). This adduct, which is observed as a side-product in the synthesis of βGlcYariv,[24] could be obtained in a preparatively useful yield by using a five-fold excess of phloroglucinol in the coupling reaction. Synthesis of the 6-deoxy-6-azido-*p*-aminophenyl-β-D-glucoside (**7**) was accomplished by Boc protection of the corresponding aniline (**1)** followed by tosylation, substitution with azide, and carbamate deprotection (Scheme 1, B). Diazotization of **7**, subsequent coupling with **3**, followed by isolation and purification using a redissolution and reprecipitation protocol afforded **AzYariv** in 18% yield (Scheme 1, C). The ^{1}H NMR spectrum of **AzYariv** (Supporting Information) indicates the presence of distinct anomeric and OH resonances

derived from the glucosyl and 6-azido glucosyl moieties. The IR spectrum of **AzYariv** displays the characteristic azide stretch at 2100 cm^{-1} (Figure S1). The CD spectrum of **AzYariv** exhibits two positive bisignate Cotton effects similar to other β-D glycosyl Yariv reagents, with a lower intensity than the parent βGlcYariv (Figure 2A). To confirm that installation of the azide does not disrupt the AGP binding of **AzYariv** we carried out reverse gel assays to determine binding. The precipitate halos formed by **AzYariv** indicate that it still binds gum arabic, although the halos are smaller than those observed for βGlcYariv, indicative of weaker binding (Figure 3, black boxes). These findings are consistent with the recently reported correlation between the magnitude of the CD signal and AGP binding ability.[16]

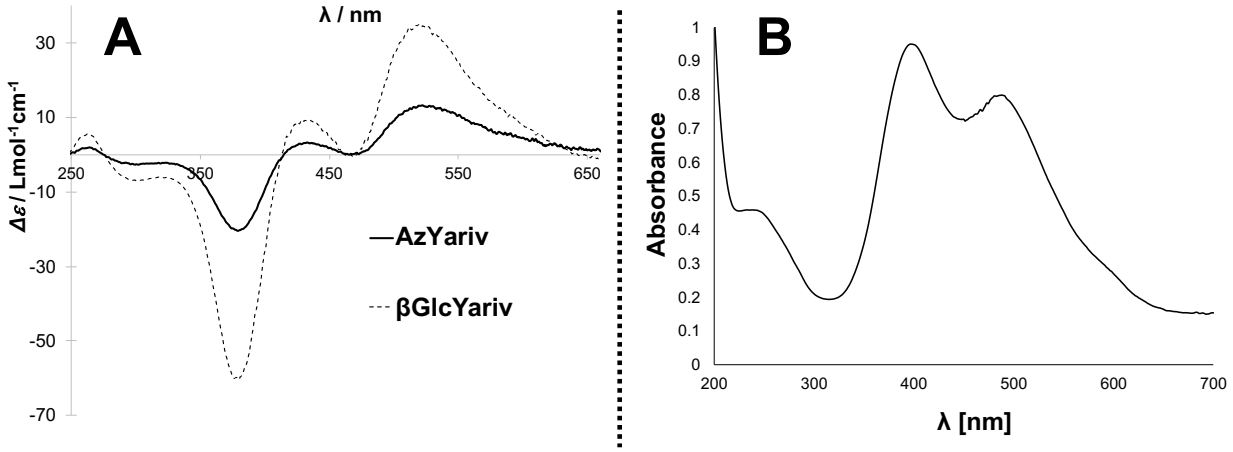

Figure 2 – A) CD spectra of **AzYariv** and βGlcYariv; B) Absorbance spectrum of **AzYariv**. All spectra obtained in water at [300 μM].

Optimization of Click Reaction Conditions

With the **AzYariv** reagent in hand, we turned our focus to the cycloaddition. The choice of fluorescent chromophore is limited by the strong 400 nm and 490 nm absorptions of the Yariv chromophore (Figure 2B). We opted to proceed with the cyanine dye Cy5, which has absorption

and emission maxima at 646 and 662 nm, respectively. The tris azo phloroglucinol Yariv chromophore does not strongly absorb at these wavelengths, reducing the potential for self-quenching. The cycloaddition of **AzYariv** with the commercially available conjugate of Cy5 linked to azodibenzocyclooctyne (**Cy5-DBCO**) was examined under a variety of solvent systems, times, and reagent ratios (Table 1). The reaction was first attempted with a 1:2 cyclooctyne:azide ratio in DMSO/water (15:85) over 16 hours. After dilution of the reaction in water and extraction with dichloromethane, we observed that the organic solution was an intense blue color, indicative of unreacted **Cy5-DBCO** (Table 1, Trial 1). Conducting the reaction for a longer time did not reduce the intensity of the blue color (Table 1, Trial 2). Increasing the ratio of DMSO (1:1) slightly reduced the blue color after work-up, suggesting that poor solubility of **Cy5-DBCO** in the reaction solution could be a factor contributing to the incomplete reaction (Table 1, Trial 3). Increasing temperature did not reduce the blue color in the organic phase, although performing the reaction in pure DMSO suggested increased conversion, as indicated by a fainter color after work-up (Table 1, Trials 4-6). Reducing the cyclooctyne:azide ratio from 1:2 to 1:5 greatly reduced the color after extraction, and after performing the reaction for 4 hours we found no blue color was washed out during extraction (Table 1, Trials 7,8). High resolution mass spectrometry of the reaction after work-up shows the expected [M^+] ion at 1780.7686 Da, along with excess unreacted **AzYariv** (Figure S2). The **AzYariv-Cy5** conjugate was not further purified, and was used as a 1:4 mixture of **AzYariv-Cy5**:**AzYariv** in subsequent mixtures.

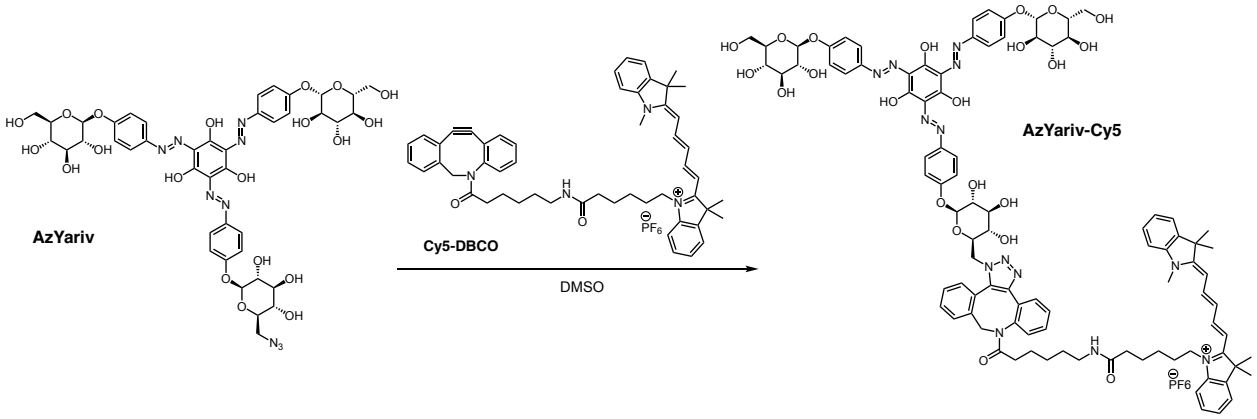

Trial	Cy5-DBCO [mM]	DMSO %	Time [hr]	Temperature [°C]	Outcome
1	0.515	15	16	25	
2	0.515	15	40	25	
3	0.515	50	16	25	
4	0.515	50	4	60	Incomplete Reaction
5	0.515	50	16	60	
6	0.515	100	16	25	
7	0.206	100	2	25	
8	0.206	100	4	25	Reaction Completion

Table 1 – Optimization of click reaction conditions between **AzYariv** and Cy5-DBCO. **AzYariv** concentration was kept at 1.03 mM.

*Agarose Gel Studies of **AzYariv-Cy5•Gum Arabic** Binding*

To evaluate the binding efficiency of the fluorescently labeled **AzYariv-Cy5** we carried out several binding experiments in agarose gels. We found **AzYariv-Cy5** does not exhibit an orange halo, indicating that it does not bind and precipitate gum arabic AGP (Figure 3). We speculate that the lack of binding of pure **AzYariv-Cy5** could arise due to the poor water solubility of AzYariv-Cy5 and/or the lack of formation of aggregates required for binding. However, when **AzYariv-Cy5** is formulated as a mixture with βGlcYariv in percentages ranging from 0.1% to 5%, precipitate formation is consistently observed.

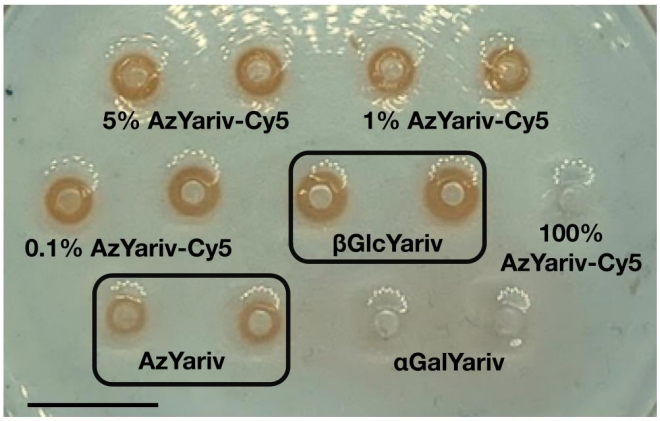

Figure 3 – Reverse gel assay with **AzYariv-Cy5** doped into βGlcYariv [1.03 mM] and relevant controls. Scale bar = 1 cm.

While the above results indicate halo formation in the reverse gel, they do not confirm that **AzYariv-Cy5** has formed co-aggregates with βGlcYariv and is present in the precipitated halos. To determine whether **AzYariv-Cy5** was present in the aggregate we imaged halos produced by the **AzYariv-Cy5**/βGlcYariv mixture using fluorescence microscopy. Examination of the halos under a fluorescent microscope indicated the presence of a fluorescent ring where precipitate could be observed visually (Figure 4). A dilution series indicated that a fluorescent ring could be observed when **AzYariv-Cy5** was present at concentrations of 100 nM and higher (Figure 4, A-C). As negative controls we evaluated the fluorescence of wells containing only βGlcYariv and **AzYariv-Cy5** independently. Gratifyingly, we found no localized fluorescence in these experiments (Figure 4, E, F). The tris α-D-galactosyl Yariv reagent (αGalYariv), a non AGP binding Yariv reagent, showed no binding and no fluorescence, as expected (Figure 4G). Furthermore, no fluorescence was observed when **AzYariv-Cy5** was added to αGalYariv (Figure 4H). The fluorescence of gels with AzYariv alone and βGlcYariv doped with Cy5-DBCO were also evaluated and found to be negligible (Figure S3). No loss of binding was observed when a gel binding assay was carried out with a sample of the **AzYariv-Cy5**/βGlcYariv mixture that had been lyophilized and reconstituted (Figure 4D). This is a significant finding, as the ability to lyophilize

and reconstitute the **AzYariv-Cy5**/βGlcYariv mixture is advantageous for storage and shipping of this reagent. We were highly encouraged by these studies showing that the **AzYariv-Cy5**/βGlcYariv combination binds to gum arabic AGP and displays bright fluorescence, so we turned our attention to imaging AGPs in plants using **AzYariv-Cy5**.

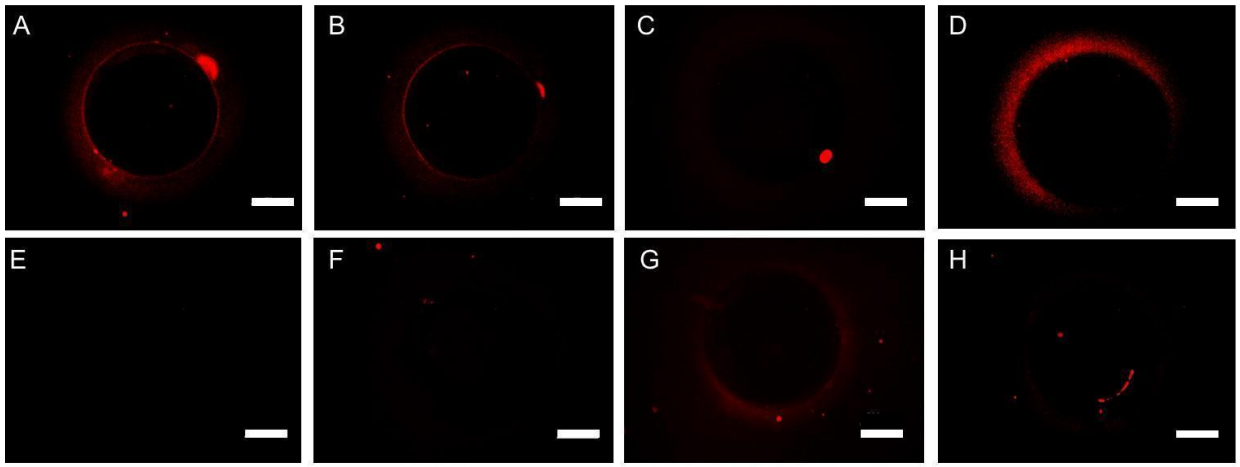

Figure 4 – Representative fluorescence images of **AzYariv-Cy5** binding in agarose reverse gels with gum arabic AGP. Concentrations of βGlcYariv and αGalYariv are 1.03 mM. **A) AzYariv-Cy5** (5 μM)/βGlcYariv, **B) AzYariv-Cy5** (100 nM)/βGlcYariv, C) **AzYariv-Cy5** (5 nM)/βGlcYariv, **D) AzYariv-Cy5** (5 μM)/βGlcYariv Lyophilized, **E)** βGlcYariv, **F) AzYariv-Cy5** (5 μM), **G)** αGalYariv, **H) AzYariv-Cy5** (5 μM)/αGalYariv. Scale bar = 500 μm.

Fluorescence Microscopy of AyYariv-Cy5 in Maize Leaves

We carried out imaging studies in maize leaves to determine the ability of **AzYariv-Cy5** to visualize AGP *in planta*. Fixed maize leaves were treated using a mixture of **AzYariv-Cy5**/βGlcYariv reagents. Fluorescence was observed in the phloem, bundle sheath, as well as epidermal cell walls, regions where AGPs are expected to be found (Figure 5). As a negative control, imaging was also carried out using **AzYariv-Cy5**/αGalYariv reagents, which do not bind AGPs, showing no labeling of these features (Figure 5). Furthermore, experiments using only βGlcYariv, where binding is expected but fluorescence is not, show results similar to **AzYariv-Cy5**/αGalYariv (Fig S5A). Leaf autofluorescence is observed in both of these negative control

experiments, but the intensity and localization differ from the fluorescence observed when **AzYariv-Cy5**/βGlcYariv is used, providing evidence for specific labeling of AGPs with the **AzYariv-Cy5** probe. Additional confirmation of the AGP binding specificity of the **AzYariv-Cy5**/βGlcYariv mixture was obtained by carrying out imaging experiments with various monoclonal antibodies (JIM4, JIM13, LM2, MAC207), corroborating the locations of AGPs in the stained samples (Figures 5 and S4). The antibodies vary slightly in their localization as they all bind to different AGP epitopes. For example, staining with LM2, which binds to oligogalactans terminated with glucuronic acid, shows weaker staining of the vasculature than staining with JIM4, for which the trisaccharide (β-D-GlcA-(1→3)-α-D-GalA-(1→2)-α-D-Rha is a strong binding epitope.[25,26] Staining with **AzYarivCy5**/βGlcYariv is stronger in the inner wall of the upper epidermal cells than any of the other antibodies tested. Additionally, the AzYarivCy5/βGlcYariv exhibits a more consistent stronger staining pattern throughout the leaf, perhaps reflecting the fact that it preferentially binds to the conserved β(1-3) galactan backbone of AGPs.

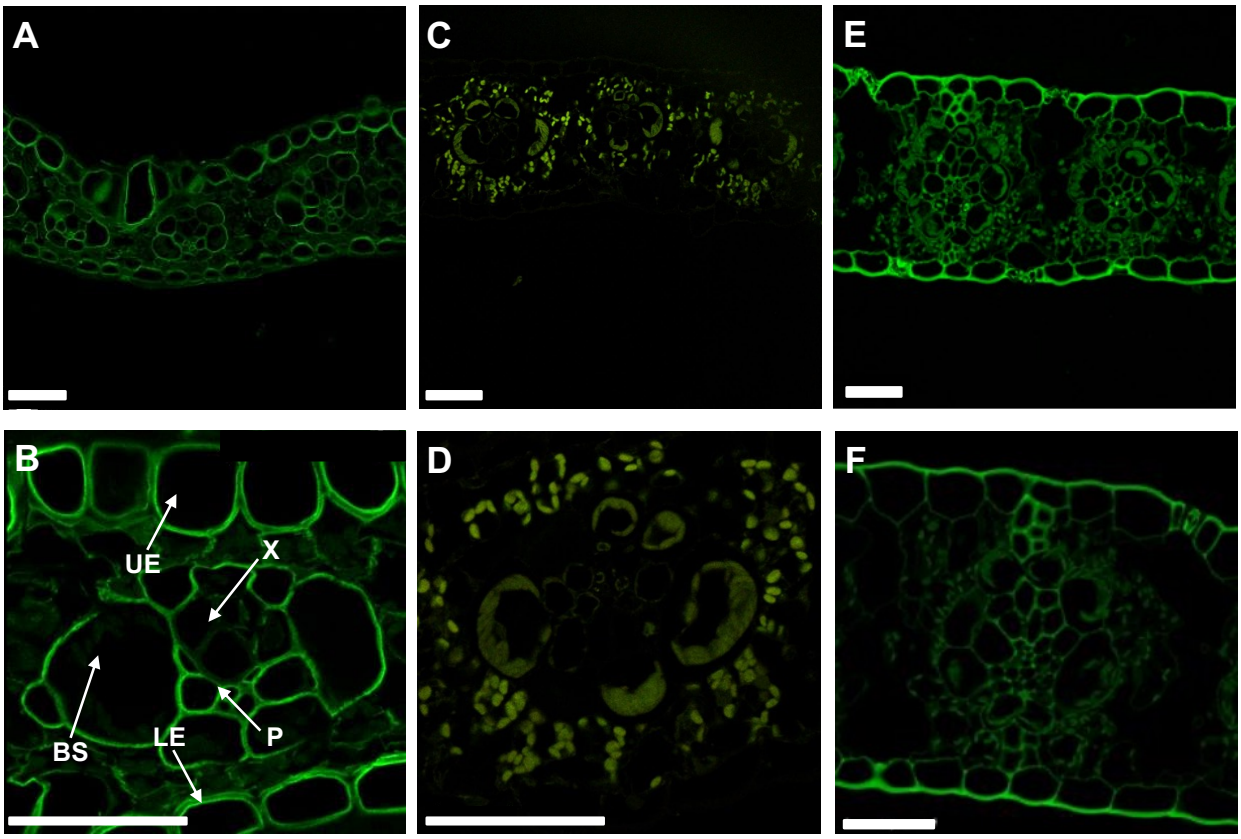

Figure 5 – Representative confocal images of fixed maize leaves treated with Yariv reagents (A-D, imaged with 651 nm laser) and antibodies (E, F, imaged with 495 nm laser). A) **AzYariv-Cy5/**βGlcYariv; B) Zoom of **AzYariv-Cy5/**βGlcYariv. UE = Upper epidermal cells, P = phloem, X = xylem, BS = Bundle sheath, LE = Lower epidermal cells.; C) **AzYariv-Cy5/**αGalYariv; D) Zoom of **AzYariv-Cy5/**αGalYariv; E) LM2; F) JIM4. Scale bar = 50 μm.

An advantage of using the Yariv reagents for visualization is the ability to perform staining experiments in fresh plant tissue.[27–29] These experiments are critical to determining AGP function in live cell assays and cannot be replicated by MAbs, which do not precipitate AGPs and require chemical fixation prior to imaging. We evaluated the ability of **AzYariv-Cy5** to stain fresh maize leaves (Figure 6). The phloem and bundle sheath are stained strongly, as is also seen with fixed leaves. Surprisingly, fluorescence from the epidermal cell walls was considerably weaker, suggesting that AGPs in these cells might become more accessible to the Yariv reagent after fixing. Autofluorescence arising from chlorophyll can be seen in these images, but this is distinct from the bright fluorescence exhibited by **AzYariv-Cy5** in the cell walls. Attempts to increase the signal

by varying staining time or prewashing the leaves were unsuccessful. Negative control experiments with both **AzYariv-Cy5**/αGalYariv and βGlcYariv both indicated no fluorescence staining of the cell walls (Figure 6 and Figure S5B Supporting Information). These findings indicate that imaging with **AzYariv-Cy5**/βGlcYariv is highly selective for AGPs, and exhibits bright fluorescence in plant cell walls.

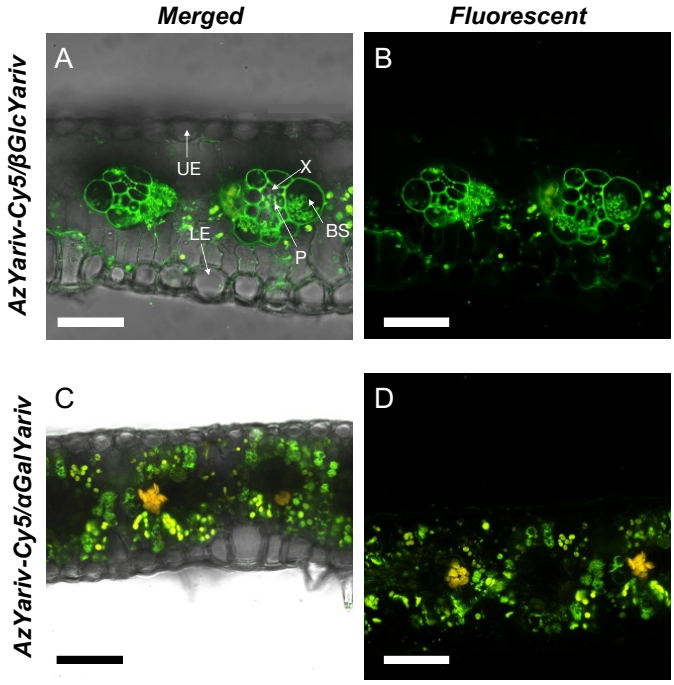

Figure 6 – Representative confocal images of fresh maize leaves treated with **AzYariv-Cy5**/βGlcYariv (top) and **AzYariv-Cy5**/αGalYariv (bottom) imaged with 651 nm laser. UE = Upper epidermal cells, P = phloem, X = xylem, BS = Bundle sheath, LE = Lower epidermal cells. Scale bar = 50 μm.

Conclusions

Small molecule probes capable of localizing polysaccharides and proteoglycans are powerful tools for unraveling the complexity of plant cell walls. We have developed the first fluorescent Yariv reagent which binds AGPs. Our preliminary results with **AzYariv-Cy5** show that these conjugated Yariv reagents, when combined with βGlcYariv, bind to gum arabic in

agarose reverse gel binding assays. The assays show fluorescence of **AzYariv-Cy5** co-localized with the precipitate ring**,** and dim or no fluorescence is seen in negative controls using **AzYariv-Cy5**/αGalYariv mixtures or non-fluorescent Yariv reagents. The utility of the **AzYariv-Cy5** reagent as a tool for plant biology is seen in the results of imaging experiments in fixed maize leaves, which show distinct fluorescence emanating from the cell walls of phloem, epidermal, and bundle sheath cells. Imaging experiments with fresh leaves also show expected binding patterns as well as bright fluorescence from cell wall staining, providing the opportunity to use the **AzYariv-Cy5** reagents for real-time imaging experiments.

Given the facility of azide functionalization using the SPAAC, there are a variety of additional conjugates of **AzYariv** that can be prepared. While the core Yariv reagent chromophore necessitates that any fluorescent chromophores that are clicked onto **AzYariv** have excitation and emission maxima at wavelengths greater than 600 nm, the presence of chlorophyll autofluorescence remains a concern at these wavelengths. The use of spectral unmixing[30] or near-infrared (NIR) dyes can reduce these artefacts. Cycloaddition of deuterated fragments can enable imaging using coherent anti-Stokes Raman scattering (CARS) microscopy, and the azide IR stretch can also be used directly for FT-IR imaging.[31,32]

Experimental Procedures

2,4-bis((E)-(4-β-D-glucosyloxyphenyl)diazenyl)benzene-1,3,5-triol (3)

Procedure modified from J. Org. Chem. ***2020****, 85, 16236–16242.*

A 250mL round bottom flask was charged with a stir bar, 4-aminophenyl-β-D-glucose **1** (408 mg, 1.51 mmol, 1 equiv.), and freshly prepared 1.2M HCl (4.0 mL). The flask was stirred in an ice

bath for 20 minutes. In a separate 2 mL Eppendorf tube sodium nitrite (106 mg, 1.54 mmol, 1 equiv.) was dissolved in water (0.3 mL) and was also placed into an ice bath. Once cooled the sodium nitrite solution was added to a 1 mL syringe fitted with a 4' 22-gauge needle clamped above the stirring reaction to perform a gravity assisted dropwise addition. The reaction was stirred at 0 °C for 2 hours. Phloroglucinol (939 mg, 7.45 mmol, 5 equiv.) was added to a 5 mL Eppendorf tube and dissolved in 5M NaOH (3 mL) and cooled in an ice bath. The phloroglucinol solution was added in one portion to the stirring diazotized sugar solution. The pH was adjusted to 10 and maintained by the addition of 5M NaOH as necessary and stirred overnight. The reaction was acidified to pH 6 by the addition of 12M HCl. After addition of HCl a thin layer of precipitated material was present along the walls of the flask. The solution was filtered through a Hirsch funnel under reduced pressure and a white solid was collected. The solid was washed with several portions of water. The solid was allowed to dry on the filter paper then discarded. The filtrate was charged with another 2 mL portion of 12 M HCl and the solution reached pH 2. Cold ethanol (200 mL) was added to the solution and a red precipitate formed; the flask was placed in a freezer for 24 hours to promote further precipitation from the solution. After 24 hours the red precipitate that was obtained was filtered through a Hirsh funnel to yield a red powder. The powder was allowed to air dry in the filter for an hour then scraped and placed into a separate pre-weighed 20 mL scintillation vial. The vial was then placed in a vacuum oven set to 75°C for 24 hours. Crude **3** (846 mg) was obtained as a fine red powder contaminated with solvent and phloroglucinol.

Redissolution and Reprecipitation

Crude **3** (400 mg) was deposited into a 500 mL Erlenmeyer flask and charged with methanol (100 mL). The solution was heated and vortexed until dissolution of the solid material. The solution was allowed to cool slightly, then charged with diethyl ether (250 mL) at which point a red

precipitate was observed. The solution was centrifuged and the supernatant was discarded. The centrifuge tube was charged with diethyl ether (10 mL) and shaken until the red powder freely floated through the centrifuge tube. The solution was filtered through a Hirsch funnel and allowed to air dry for 1 hour. The resulting dark red solid was transferred to a pre-weighed 1-dram vial and placed into a vacuum oven set to 75°C. The **R1 3** (360 mg, 90%) was obtained as a dark red powder. A second redissolution and reprecipitation was performed on the **R1** material with 75 mL of methanol and 150 mL of diethyl ether to yield **R2 3** (259 mg, 0.38 mmol, 72%) as a dark red powder. ^{1}H NMR (600 MHz, DMSO-d_6) δ 15.57 (s, 1H, core Ar-O*H*), 7.61 (d, *J* = 8.4 Hz, 4H, Ar-C*H ortho* to sugar), 7.15 – 7.10 (m, 4H, Ar-C*H ortho* to azo), 5.77 (s, 1H, core Ar-C*H*), 5.34 (d, *J* = 4.8 Hz, 2H, 2-O*H*), 5.10 (s, 2H, 3-O*H*), 5.03 (d, *J* = 5.1 Hz, 2H, 4-O*H*),) 4.89 (d, *J* = 7.7 Hz, 2H, *H1*),4.59 (s, 2H, 6-O*H*), 3.68 (dd, *J* = 12.1, 2.1 Hz, 2H, $H6_a$), 3.48 (dd, *J* = 12.0, 5.6 Hz, 2H, $H6_b$), 3.34 (ddd, *J* = 9.9, 4.8, 2.7 Hz, 1H, *H5*), 3.31 (t, *J* = 8.9 Hz, 2H, *H3*), 3.24 (dd, *J* = 9.0, 7.7 Hz, 2H, *H2*), 3.18 (t, *J* = 9.2 Hz, 2H, H4). ^{13}C NMR (151 MHz, DMSO-d_6) δ 176.8 (Core Ar, *C*=O), 155.8 (Ar, *C*-O-Sugar), 136.2 (Ar, *C*-N), 118.1 (Ar, *C*-C-N), 117.4 (Ar, *C*-C-O-Sugar), 101.6 (Core Ar, *C*H), 100.6 (*C*1), 77.1 (*C*5), 76.6 (*C*3), 73.3 (*C*2), 69.7 (*C*4), 60.7 (*C*6). HRMS (+ESI) *m/z* $[M+H]^+$ calcd for $C_{30}H_{35}N_4O_{15}$ 691.2093, found 691.2093.

AzYariv

A 25 mL round bottom flask containing crude *p*-aminophenyl-6-deoxy-6-azido-β-D-glucopyranoside trifluoroacetate (107 mg, 0.26 mmol, 1 equiv.) was charged with a stir bar and freshly prepared 1.2 M HCl (1.5 mL). The flask was placed into a salt and ice bath at 0°C and allowed to stir for 15 minutes. In a separate 2 mL Eppendorf tube sodium nitrite (20 mg, 0.29 mmol, 1.1 equiv.) was dissolved in water (0.25 mL) and placed into an ice bath. Once cool the

nitrite solution was added to a syringe fitted with a 4" 22-gauge needle clamped above the stirring solution and allowed to drip into the reaction solution. The reaction was allowed to stir at 0 °C for 2 hours. After 2 hours a 2 mL Eppendorf tube was charged with **3** (180 mg, 0.26 mmol, 1 equiv.) and dissolved in 2M NaOH (1.5 mL), the tube was then cooled to 0°C. Once cooled the Yariv solution was added dropwise to the stirring diazotized azido sugar solution over a period of 10 minutes. The solution which was at pH 5 after the addition was brought to pH 10 by the addition of 5M NaOH. The reaction was allowed to reach room temperature and stirred overnight. After 18 hours of stirring the dark red reaction read pH 10. The solution was transferred to a 250 mL Erlenmeyer flask and acidified to pH 2 by the addition of 12 M HCl. 95% Ethanol (60 mL) was then added to the flask and a fine dark red precipitate formed in the solution. The flask was covered with parafilm and placed in a freezer for 24 hours to promote further precipitation from the solution. The solution was filtered under reduced pressure through a Hirsch funnel. The resulting dark red solid was allowed to dry for an hour in the filter before being crushed into a fine powder and transferred to a pre-weighed 20 mL scintillation vial. The vial was then placed into a vacuum oven next to a beaker with Drierite™ and dried overnight at room temperature. The crude **AzYariv** reagent (290 mg) was obtained as a fine dark red powder. Contaminated with EtOH and water.

Redissolution and Reprecipitation

The crude **AzYariv** reagent (290 mg) was added to a 50 mL round bottom flask and dissolved in water (3 mL) while heating and vortexing. Cold 95% ethanol (50 mL) was then added to the solution and a dark red precipitate crashed out of solution. The solution was filtered through a Hirsch funnel under reduced pressure and allowed to air dry for an hour in the funnel. The powder

was then transferred to a pre-weighed 20 mL scintillation vial. The R1X **AzYariv** reagent (140 mg, 48%) was obtained as a dark red powder.

Trituration with Methanol

The R1X **AzYariv** reagent (140 mg) was added to a 25 mL round bottom flask and charged with boiling methanol (5 mL). The solution was filtered through a Hirsch funnel. The resulting black powder was further washed with 4 portions of boiling methanol (5 mL). The black powder was allowed to air dry in the funnel for 1 hour before being scraped into a pre-weighed 20 mL scintillation vial and being stored in a desiccator. The R1XM **AzYariv** reagent (47 mg, 36%, 18% from starting material) was obtained as a fine black powder. ^{1}H NMR (600 MHz, DMSO-d_6) δ 15.92 – 15.87 (m, 3H, core Ar-O*H*), 7.69 – 7.66 (m, 6H, Glc Ar-*H ortho* to azo & AzGlc Ar-*H ortho* to azo), 7.19 (m, 6H, Glc Ar-*H ortho* to sugar & AzGlc Ar-*H ortho* to sugar), 5.50 (d, *J* = 5.0 Hz, 1H, AzGlc C2-O*H*), 5.45 (d, *J* = 5.1 Hz, 1H, AzGlc C4-O*H*), 5.40 (d, *J* = 5.0 Hz, 2H, Glc C2-O*H*), 5.36 (d, *J* = 4.5 Hz, 1H, AzGlc C3-O*H*), 5.23 (d, *J* = 4.3 Hz, 2H, Glc C3-O*H*), 5.18 (d, *J* = 4.9 Hz, 2H, Glc C4-O*H*), 5.06 (d, *J* = 7.7 Hz, 1H, AzGlc *H1*), 4.93 (d, *J* = 7.7 Hz, 2H, Glc *H1*), 4.67 (t, *J* = 5.9 Hz, 2H, Glc C6-O*H*), 3.69 (s, 4H, Glc *H6$_a$*), 3.66 (d, *J* = 9.7 Hz, 1H, AzGlc *H5*), 3.54 – 3.48 (m, 3H, Glc *H6$_b$* & *AzGlc H6$_a$*), 3.45 (dd, *J* = 13.3, 7.3 Hz, 2H, Az Glc H6$_b$), 3.34 – 3.12 (m, 11H, Glc *H2*, *H3*, *H4*, & *H5*; AzGlc *H2*, *H3*, *H4*).^{13}C NMR (151 MHz, DMSO-d_6) δ 177.7 (Core Ar-*C*O), 156.4 (Ar-*C*-Glc), 156.0 (Ar-*C*-AzGlc), 136.2 (AzGlc-Ar-*C*-Azo), 136.0 (Glc-Ar-*C*-Azo), 128.4 (Core Ar-*C*-N), 118.5 (AzGlc and Glc Ar-*C*-C-N), 117.5 (AzGlc and Glc Ar-*C*-C-O-sugar), 100.5 (Glc *C1*), 100.1 (AzGlc *C1*), 77.1 (Glc *C5*), 76.6 (Glc *C3*), 76.1 (AzGlc *C5*), 75.1 (AzGlc *C3*), 73.3 (Glc *C2*), 73.1 (AzGlc *C2*), 70.7 (Glc *C4*), 69.6 (AzGlc *C4*), 60.6 (Glc *C6*), 51.4 (AzGlc *C6*). HRMS (+ESI) *m/z* $[M+H]^+$ calcd for $C_{42}H_{47}N_9O_{20}$ 998.3016, found 998.3002. ATR-IR cm^{-1} 2200w (Azide Stretch).

AzYariv-Cy5

A 200 μL PCR tube was charged with a 2.06 mM DMSO stock solution of AzYariv reagent (5 μL, 1.03 mM final concentration), a 2.9 mM DMSO stock solution of Cy5-DBCO (0.71 μL, 206 μM final concentration), and DMSO (4.29 μL). The tube was wrapped in foil to protect from light and allowed to stand for 20 hours. The PCR tube was then charged with water (75 μL) and DMSO (25 μL) then added to a 1.5 mL Eppendorf tube. The solution was washed three times with methylene chloride (100 μL) and the aqueous phase was added to a 1-dram vial and lyophilized to a powder. The vial was wrapped in foil to protect from light and placed into a freezer for storage. The AzYariv-Cy5 conjugate was not further purified and used as a 1:4 mixture of **AzYariv-Cy5**:**AzYariv**. HRMS (+ESI) *m/z* $[M]^+$ calcd for $C_{95}H_{106}N_{13}O_{22}$ 1780.7570, found 1780.7896.

B. Gel Binding Assays

General Procedure for the Preparation of Agarose Reverse Gels

A 25 mL Erlenmeyer flask was charged with agarose (50 mg), NaCl (35 mg) and a 1 mg/mL stock solution of gum arabic AGP (250 μL). This was then diluted to 0.05 mg/mL by the addition of water (4.75 mL). The solution was heated in a microwave oven until boiling then charged with a 0.02 (%w/v) NaN_3 solution (50 μL). The hot solution was then pipetted into a 12-well microplate (750 μL per well) using a p200 micropipette to prevent formation of bubbles. A custom made 7-pin well mold was then affixed into the gel to create wells for the Yariv reagent to be added. The well molds were removed after 10 minutes once the gels were set. Solutions of the Yariv reagent were added to the wells using a 2.5 μL Hamilton Microlite^{TM} PCG Syringe. Wells were charged

with the appropriate volume of Yariv reagent (1 μL for most solutions, 1.5 μL for pure AzYariv reagent) then the gels were placed on a platform in a water basin to prevent the gels drying out. The gels were incubated overnight for 16 hours before imaging. Gels were imaged on the Keyence All-in-One Fluorescence Microscope (BZ-X810) using the Texas Red filter (red channel) (Ex: 560/40; Em: 630/75).

Preparation of Lyophilized βGlcYariv/AzYariv-Cy5 Mixtures

Lyophilized AzYariv-Cy5 was charged with DMSO (20 μL), a 2.06 mM solution of βGlcYariv in water (103 μL), and water (83 μL). The samples were then apportioned out into 23 PCR tubes (17 μL each). The PCR tubes were fixed into a holder then the holder was placed into a large lyophilizer flask. The samples were lyophilized overnight then removed, capped, and placed into a 50 mL centrifuge tube containing Drierite™. The centrifuge tube was then sealed with parafilm and wrapped in aluminum foil to protect them from light.

C. Maize Leaf Staining and Imaging

General Procedure for Tissue Preparation and Histology

Chemically fixed tissue samples were prepared from mature maize leaf tissue by vacuum infiltration in a paraformaldehyde-based fixative solution and embedded in paraffin blocks as described previously.[33] Microtome-sectioned (8um sections) tissue was deparaffinized and rehydrated in an ethanol-water gradient series as described by Ruzin.[34] Fresh tissue was processed by hand sectioning mature maize leaf tissue under a dissection scope. Yariv staining of fresh and fixed tissue sections was performed by incubation of tissue sections on microscope slides for 4 hours (fresh material) or 16 hours (fixed material). Cy5 labeled Az-Yariv was diluted to 1μm in a

0.1mM solution of either βGlcYariv (binding) or αGalYariv as a non-binding fluorescent control. A solution of 0.1mM βGlcYariv without the Cy5 conjugated AzYariv spike-in was used as an additional control for these experiments.

Immunohistochemistry was performed according to Tsuda and Chuck.[35] Monoclonal antibodies JIM13, LM2, JIM4 and MAC207 were sourced from University of Georgia Complex Carbohydrate Research Center. Primary antibodies were diluted 1:10 and incubated for 1 hr at room temperature; secondary antibodies were diluted 1:100 and incubated for 2 hrs at room temperature. Samples were mounted in CitiFluor AF1 mounting media (Electron Microscopy Sciences, Hatfield PA).

General Procedure for Confocal Microscopy of Maize Tissue Samples

All samples were imaged on a Leica TCS SP8 confocal microscope system (Leica Microsystems, Germany) at the University of Missouri Advanced Light Microscopy Core facility. Identical microscope settings were used for each fluorescent probe and their respective controls. Cy5 labeled samples were imaged on a 20x dry objective or a 40x water immersion objective using 651 nm excitation laser, collecting fluorescence signal between 660 and 700 nm with a 1.0 AU pinhole diameter. FITC labeled samples were imaged on a 40x water immersion objective using an excitation wavelength of 495 nm, collecting emission between 505 and 540 nm.

Acknowledgements

This work was supported by awards to AB from the National Science Foundation (CHE1607554 & CHE 2203892). CD spectra were obtained at the RI NSF/EPSCoR Proteomics Shared Resource

Facility, supported by the National Science Foundation (EPSCoR 1004057), National Institutes of Health (1S10RR020923, S10RR027027), the Rhode Island Science and Technology Advisory Council, and the Brown University Division of Biology and Medicine. We thank Professor Ming Xian for the use of his fluorescence microscope.

Notes

AB and SR have filed a patent application for compounds disclosed in this manuscript.

ASSOCIATED CONTENT

Supporting Information

Experimental details for synthesis of monosaccharide precursors and protocols for gel binding assays and microscopy; ^{1}H and ^{13}C NMR spectra. This material is available free of charge on the ACS Publications website.

References

(1) Cosgrove, D. J. Growth of the Plant Cell Wall. *Nat Rev Mol Cell Biol* **2005**, *6*, 850–861.
(2) Doblin, M. S.; Pettolino, F.; Bacic, A. Plant Cell Walls: The Skeleton of the Plant World. *Functional Plant Biol.* **2010**, *37*, 357.
(3) Burton, R. A.; Gidley, M. J.; Fincher, G. B. Heterogeneity in the Chemistry, Structure and Function of Plant Cell Walls. *Nat Chem Biol* **2010**, *6*, 724–732.
(4) Zhang, B.; Gao, Y.; Zhang, L.; Zhou, Y. The Plant Cell Wall: Biosynthesis, Construction, and Functions. *Journal of Integrative Plant Biology* **2021**, *63*, 251–272.
(5) Wallace, I. S.; Anderson, C. T. Small Molecule Probes for Plant Cell Wall Polysaccharide Imaging. *Front Plant Sci* **2012**, *3*, 89.
(6) Rydahl, M. G.; Hansen, A. R.; Kračun, S. K.; Mravec, J. Report on the Current Inventory of the Toolbox for Plant Cell Wall Analysis: Proteinaceous and Small Molecular Probes. *Front Plant Sci* **2018**, *9*, 36–20.
(7) Voiniciuc, C.; Pauly, M.; Usadel, B. Monitoring Polysaccharide Dynamics in the Plant Cell Wall. *Plant Physiol* **2018**, *176* (4), 2590–2600.
(8) DeVree, B. T.; Steiner, L. M.; Głazowska, S.; Ruhnow, F.; Herburger, K.; Persson, S.; Mravec, J. Current and Future Advances in Fluorescence-Based Visualization of Plant Cell Wall Components and Cell Wall Biosynthetic Machineries. *Biotechnology for Biofuels* **2021**, *14*, 78.
(9) Classen, B.; Baumann, A.; Utermoehlen, J. Arabinogalactan-Proteins in Spore-Producing Land Plants. *Carbohydrate Polymers* **2019**, *210*, 215–224.
(10) Hromadová, D.; Soukup, A.; Tylová, E. Arabinogalactan Proteins in Plant Roots – An Update on Possible Functions. *Frontiers in Plant Science* **2021**, *12:674010*.
(11) Seifert, G. J. On the Potential Function of Type II Arabinogalactan O-Glycosylation in Regulating the Fate of Plant Secretory Proteins. *Frontiers in Plant Science* **2020**, *11:563735*.
(12) Tan, L.; Showalter, A. M.; Egelund, J.; Hernandez-Sanchez, A.; Doblin, M. S.; Bacic, A. Arabinogalactan-Proteins and the Research Challenges for These Enigmatic Plant Cell Surface Proteoglycans. *Front Plant Sci* **2012**, *3*. doi: 10.3389/fpls.2012.00140
(13) Saeidy, S.; Petera, B.; Pierre, G.; Fenoradosoa, T. A.; Djomdi, D.; Michaud, P.; Delattre, C. Plants Arabinogalactans: From Structures to Physico-Chemical and Biological Properties. *Biotechnology Advances* **2021**, *53*, 107771.
(14) Leszczuk, A.; Kalaitzis, P.; Kulik, J.; Zdunek, A. Review: Structure and Modifications of Arabinogalactan Proteins (AGPs). *BMC Plant Biology* **2023**, *23* (1), 45.
(15) Jermyn, M. A. Comparative Specificity of Concanavalin-a and Beta-Lectins. *Aust J Plant Physio.* **1978**, *5*, 687–696.
(16) Hoshing, R.; Leeber, B. W.; Kuhn, H.; Caianiello, D.; Dale, B.; Saladino, M.; Lusi, R.; Palaychuk, N.; Weingarten, S.; Basu, A. The Chirality of Aggregated Yariv Reagents Correlates with Their AGP-Binding Ability. *ChemBioChem* **2022**, *23*, e202100532.
(17) Yariv, J.; Lis, H.; Katchalski, E. Precipitation of Arabic Acid and Some Seed Polysaccharides by Glycosylphenylazo Dyes. *Biochem J* **1967**, *105*, 1C-2C.
(18) Jermyn, M. A.; Yeow, Y. M.; Woods, E. F. A Class of Lectins Present in the Tissues of Seed Plants. *Aust J Plant Physio.* **1975**, *2*, 501-531.

(19) Clarke, A. E.; Gleeson, P. A.; Jermyn, M. A.; Knox, R. B. Characterization and Localization of β-Lectins in Lower and Higher Plants. *Functional Plant Biology* **1978**, *5*, 707–722.
(20) Kitazawa, K.; Tryfona, T.; Yoshimi, Y.; Hayashi, Y.; Kawauchi, S.; Antonov, L.; Tanaka, H.; Takahashi, T.; Kaneko, S.; Dupree, P.; Tsumuraya, Y.; Kotake, T. β-Galactosyl Yariv Reagent Binds to the β-1,3-Galactan of Arabinogalactan Proteins. *Plant Physiol* **2013**, *161*, 1117–1126.
(21) Rodionova, A.; Vavříková, A.; Spiwok, V.; 2021. Structural Basis of the Function of Yariv Reagent-An Important Tool to Study Arabinogalactan Proteins. *Frontiers in Plant Science* **2021** 8:682858.
(22) Dommerholt, J.; Rutjes, F. P. J. T.; van Delft, F. L. Strain-Promoted 1,3-Dipolar Cycloaddition of Cycloalkynes and Organic Azides. *Top Curr Chem* **2016**, *374*, 16.
(23) Lombardi, L.; Sebastiani, L. Copper Toxicity in Prunus Cerasifera: Growth and Antioxidant Enzymes Responses of in Vitro Grown Plants. *Plant Science* **2005**, *168*, 797–802.
(24) Hoshing, R.; Saladino, M.; Kuhn, H.; Caianiello, D.; Lusi, R. F.; Basu, A. An Improved Protocol for the Synthesis and Purification of Yariv Reagents. *J Org Chem* **2020**, *85*, 16236–16242.
(25) Ruprecht, C.; Bartetzko, M. P.; Senf, D.; Dallabernadina, P.; Boos, I.; Andersen, M. C. F.; Kotake, T.; Knox, J. P.; Hahn, M. G.; Clausen, M. H.; Pfrengle, F. A Synthetic Glycan Microarray Enables Epitope Mapping of Plant Cell Wall Glycan-Directed Antibodies. *Plant Physiol.* **2017**, *175*, 1094–1104.
(26) Yates, E. A.; Valdor, J.-F.; Haslam, S. M.; Morris, H. R.; Dell, A.; Mackie, W.; Knox, J. P. Characterization of Carbohydrate Structural Features Recognized by Anti-Arabinogalactan-Protein Monoclonal Antibodies. *Glycobiology* **1996**, *6*, 131–139.
(27) Willats, W. G.; Knox, J. P. A Role for Arabinogalactan-Proteins in Plant Cell Expansion: Evidence from Studies on the Interaction of Beta-Glucosyl Yariv Reagent with Seedlings of Arabidopsis Thaliana. *Plant J* **1996**, *9*, 919–925.
(28) Jauh, G. Y.; Lord, E. M. Localization of Pectins and Arabinogalactan-Proteins in Lily (Lilium Longiflorum L.) Pollen Tube and Style, and Their Possible Roles in Pollination. *Planta* **1996**, *199*, 251–261.
(29) Leszczuk, A.; Kozioł, A.; Szczuka, E.; Zdunek, A. Analysis of AGP Contribution to the Dynamic Assembly and Mechanical Properties of Cell Wall during Pollen Tube Growth. *Plant Science* **2019**, *281*, 9–18.
(30) Acuña-Rodriguez, J. P.; Mena-Vega, J. P.; Argüello-Miranda, O. Live-Cell Fluorescence Spectral Imaging as a Data Science Challenge. *Biophys Rev* **2022**, *14*, 579–597.
(31) Schulz, H.; Baranska, M. Identification and Quantification of Valuable Plant Substances by IR and Raman Spectroscopy. *Vibrational Spectroscopy* **2007**, *43*, 13–25.
(32) Zhao, Y.; Man, Y.; Wen, J.; Guo, Y.; Lin, J. Advances in Imaging Plant Cell Walls. *Trends in Plant Science* **2019**, *24*, 867–878.
(33) Julius, B. T.; McCubbin, T. J.; Mertz, R. A.; Baert, N.; Knoblauch, J.; Grant, D. G.; Conner, K.; Bihmidine, S.; Chomet, P.; Wagner, R.; Woessner, J.; Grote, K.; Peevers, J.; Slewinski, T. L.; McCann, M. C.; Carpita, N. C.; Knoblauch, M.; Braun, D. M. Maize Brittle Stalk2-Like3, Encoding a COBRA Protein, Functions in Cell Wall Formation and Carbohydrate Partitioning. *The Plant Cell* **2021**, *33*, 3348–3366.
(34) Ruzin, S. E. *Plant Microtechnique and Microscopy*; Oxford University Press, 1999.

(35) Tsuda, K.; Chuck, G. Heat Induced Epitope Retrieval (HIER) Assisted Protein Immunostaining in Maize. *Bio-protocol* **2019**, *9* (11), e3260.

TOC Graphic

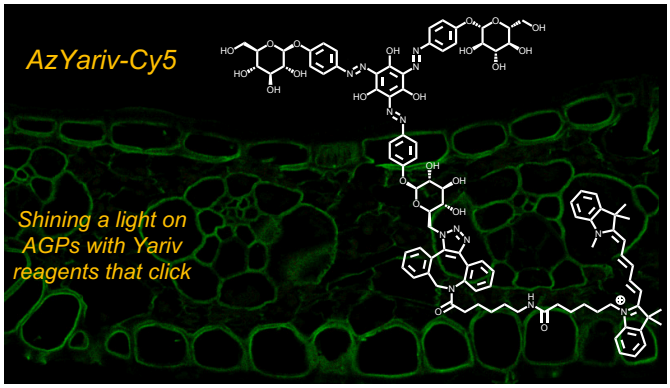
AzYariv-Cy5
Shining a light on AGPs with Yariv reagents that click